The 2009 IEEE/RSJ International Conference on
Intelligent Robots and Systems
October 11-15, 2009 St. Louis, USA

Windshield Shape Inspection Using Structured Light Patterns from Two Diffuse Planar Light Sources

Jing Xu, Ning Xi, Chi Zhang and Quan Shi

Abstract— **The objective of this paper is to propose a windshield surface shape and optical parameters inspection system. In this paper, a white board works as a diffuse planar light source projecting structured light patterns because physical properties of specular surface do not allow us to directly apply the triangulation-based techniques used in ordinary diffuse surface inspection. The board is placed at two different positions and the distorted structured light patterns are observed by a fixed camera so that the incident vector for every point on the windshield surface is determined using corresponding points in the board at two different positions. Likewise, the reflection vector is determined by camera calibration. Hence, the 3D shape and normal of the windshield surface are obtained by the intersection of the incident and reflection vectors. The normal of the surface denotes the optical reflective property of the windshield. Last, accuracy and consistence experiments are conducted. The experiment results demonstrate the efficiency and accuracy of our system.**

I. INTRODUCTION

There is an increasing requirement to quickly measure the 3D shapes and optical parameters of glass in automotive manufacturing industries. However, physical properties of specular surface do not allow us to apply the triangulation-based techniques for measuring a specular surface. The reason is that the projected light is only reflected to one single direction and little light can reach the camera. The traditional method of structured light technique only can measure the diffuse surface. As a result, the windshield surface is painted with powder or other material before being measured. Therefore, it reduces inspection speed and increases the inspection error due to the material covered on the surface [1], [2].

A promising method for directly inspecting the specular surface is to move the light source or camera position in the procedure of measurement [3]. The disadvantage for this method is that it is difficult to obtain high resolution because each light source should be viewed by the camera . As a result it takes a long time to finish the measurement. Therefore, it is not suitable for inspecting a large scale surface. To overcome such limitation, a diffusive screen of a planar light source is introduced as a structured light source so that the entire surface information can be captured by one camera [4]- [7]. Common strategy for such measurement systems is based on the observation of distorted structured patterns which are reflected by the inspected part surface. The phase distribution for the structured patterns is obtained and the relation between slope distribution and the height distribution of the specular surface can be obtain. In this case, the 3D shape of the specular surface is caculated by integrating the slope distributions from several known position points. However, the random errors will accumulate and result in measurement error while performing a numerical integration. By assuming that the surface is a plane locally, normal vectors of the surface are determined from eight neighbor pixels and the 3D shape surface is reconstructed [8].

In this paper, a method of inspecting specular surface is proposed. For this purpose, a white board working as a planar light source is placed at two different positions through which the incident ray for every windshield surface point can be obtained. In addition, the reflected ray for every windshield surface point can be determined from camera calibration; hence, we can compute the position and normal for every windshield surface point. Similar research is conducted in [9].

The remaining sections of this paper are arranged as follows: in section II, the overall system is introduced. As well, the inspection geometry is described and the system error is analyzed . The calibrations of sensors and system are given in section III. In section IV, the accuracy and consistency of the measurement system are tested. The conclusion is given in section V.

II. INSPECTION PRINCIPLE

A. Inspection System

Considering the reflection properties of the specular surface, it is obviously that a point light source such as Digital Light Procession (DLP) projection is not suitable. Instead, a diffuse planar light is necessary for constructing fringe patterns. As shown in Fig.1, a projection screen is used. Each point will project structured light to the windshield surface. In this case, there is one point on the screen corresponding to the pixel in the camera. Additionally, a virtual image, called a 'back image' is generated. Therefore, for a fixed camera, there is one incident light from a point in the view region detected. This method, for measuring a specular surface is also called a 'Back-image' method.

The triangulation-based 3D measurement method only has one unknown variable to solve, surface position . However, there are two variables needed to be solved simultaneous for specular surface, they are surface position and normal. Hence, a second planar light source is introduced in our

Jing Xu, Ning Xi, Chi Zhang are with Department of Department of Electrical and Computer Engineering, Michigan State University, East Lansing, MI, 48824, USA; xujing08@msu.edu; xin@egr.msu.edu; zhangc11@msu.edu

Quan Shi is with PPG Industries Inc., Glass Research Center, 400 Guys Run Road. Cheswick, PA, 15024, USA. qshi@ppg.com

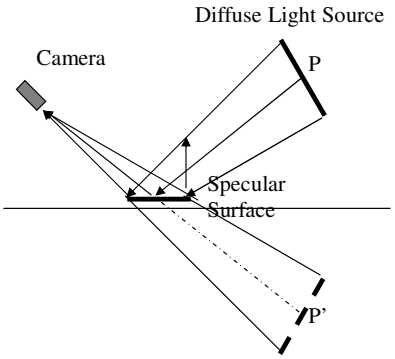

Fig. 1. Specular surface inspection using diffuse light source

system as a constrained condition. The principle of the measurement system is described below.

The system for inspecting windshield consists of a computer, a Charge Coupled Device (CCD) camera, a DLP projector and a white board which is show in Fig.2. When measuring the windshield surface, a group of structured light patterns are generated in the computer and transmitted to the projector. The projector projects the fringe patterns to the white board which is regarded as a diffuse planar light source relative to the windshield. Then, the camera captures the distorted patterns to obtain the corresponding pixel position in the white board for every windshield surface point . After, the board is placed in a different position. Projecting patterns and capturing distorted ones are carried out again so that there are two point positions in the incident ray for every windshield point. For example, for point P, we can find out P_1 and P_2 in the Fig.2. Therefore, we can obtain the incident ray through the planar light source in two different positions. Additionally, the reflected ray can be obtained by camera calibration. In this case, the position and normal for every surface point are determined by the intersection of the incident ray and reflected ray.

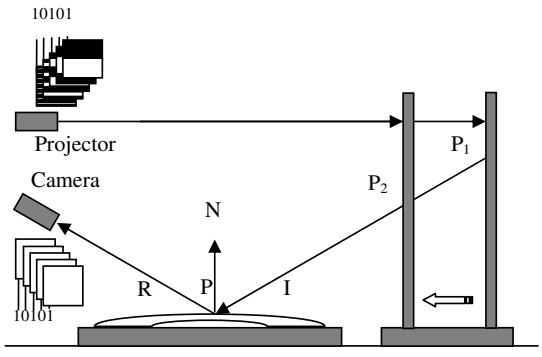

Fig. 2. The inspection principle

B. Structured Light Pattern

The Phase Shifting method is a common solution to obtain the shape of the surface. To measure a discontinuous surface, the Gray Code method can be applied for unwrapping the calculated phase map, called GCPS method [10]. However, for a sinusoid wave, at the area of the peak and valley, the magnitude does not have significant variation with phase value. Random noise may easily increase the error of a derived phase map. Considering the intensity noise, a square wave is much more robust than a sinusoid, Such a method, named GCLS (Gray Code and Line Shifting) is used for 3D shape measurement. Furthermore, sub-pixel measurement can also be achieved using GCLS [2]. An edge detection method is shown in Fig.3 using another image with an opposite intensity strip. A, B, C and D denote the intensity values in the pixel n and n+1. The location of a stripe boundary can be represented by:

$$P = P_{n+1} - \frac{D-B}{(A+D)-(B+C)} \tag{1}$$

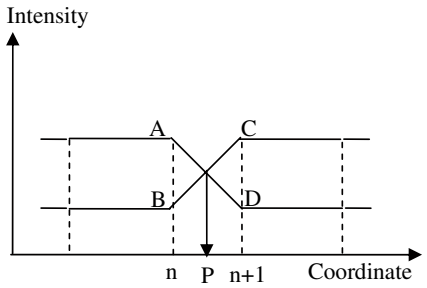

Fig. 3. The edge detection

When vertical CGLS fringe pattern is used, the vertical coordinate for every point on the white board is obtained. Likewise, when horizontal verision is used, the horizontal coordinate for every point on the white board is obtained. To determine the incident vector, the vertical and horizontal coordinates for every point on the board are both needed so that the vertical and horizontal CGLS fringe patterns are projected at each position shown in Fig.4.

The resolution of our projector is 1024×768 pixels. In practice, six patterns are used to produce 64 vertical strips so that each stripe has 16 pixels. Then each stripe is shifted 16 times to generate $64 \times 16 = 1024$ codes. Likewise, six patterns are used to produce 64 horizontal strips so that each stripe has 12 pixels. And each strip should be shifted 12 times to generate $64 \times 12 = 768$ codes.

The drawback of GCLS method is that it needs more images than GCPS method to obtain required point density, which slows the measurement process. However, for inspection, the measurement accuracy and measurement precision are more important. Therefore, The GCLS method is used in this paper.

Fig. 4. The vertical and horizontal patterns

C. Geometry of the Inspection

Now we will discuss how to compute the unknown 3D point position and corresponding normal for every point on the surface by the calibrated camera and the calibrated patterns on two white boards. The camera model is expressed as follows [11]:

$$s\begin{bmatrix} r \\ c \\ 1 \end{bmatrix} = \begin{bmatrix} m_{11} & m_{12} & m_{13} & m_{14} \\ m_{21} & m_{22} & m_{23} & m_{24} \\ m_{31} & m_{32} & m_{33} & 1 \end{bmatrix} \begin{bmatrix} x \\ y \\ z \\ 1 \end{bmatrix} \tag{2}$$

Where s is a scale factor;$[r,c,1]^T$is the homogeneous coordinate of the pixel in the image frame;$[x,y,z,1]^T$ is the homogeneous coordinate of the corresponding point in reflected ray in the world frame; $\begin{bmatrix} m_{11} & m_{12} & m_{13} & m_{14} \\ m_{21} & m_{22} & m_{23} & m_{24} \\ m_{31} & m_{32} & m_{33} & 1 \end{bmatrix}$ is the matrix product of the camera extrinsic parameters matrix and intrinsic parameters matrix which are obtained by camera calibration.

Eliminating the homogeneous scale s in equation (2), we obtain the reflected ray equation by the following liner equation:

$$\begin{cases} r = (m_{11} - m_{31}r)x + (m_{12} - m_{32}r)y + (m_{13} - m_{33}r)z + m_{14} \\ c = (m_{21} - m_{31}c)x + (m_{22} - m_{32}c)y + (m_{23} - m_{33}c)z + m_{24} \end{cases} \tag{3}$$

The incident ray equation can be written as:

$$\begin{cases} \frac{x-x_1}{x_2-x_1} = \frac{y-y_1}{y_2-y_1} \\ \frac{y-y_1}{y_2-y_1} = \frac{z-z_1}{z_2-z_1} \end{cases} \tag{4}$$

Where (x_1,y_1,z_1) is the coordinate of the point on the board in first position in the world frame; (x_2,y_2,z_2) is the coordinate of the corresponding point on the board in second position in the world frame. (x,y,z) is the coordinate of the any point on the incident ray.

Combining equations (3) and (4), we can get the coordinate of the windshield surface point. The equation can be solve by least squares. However, due to errors in camera model and point position on the board, the two rays will not intersect in the 3D space. The better way is to computer the shortest line segment connecting them shown in Fig.5. If the length of this segment is less than the threshold, we can assign the midpoints as the intersection of the two lines. If it is greater than the threshold, we assume that there are some mistakes for corresponding points in the camera image and on the white board.

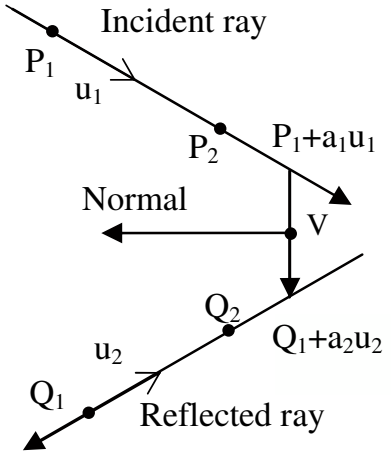

Fig. 5. The shortest distance between two skew lines

In Fig.5, P_1 and P_2 are the points on the board; Q_1 and Q_2 are those in the reflected ray and often are the optical center of the camera and the image plane points; u_1 and u_2 are the unit vectors ; V is the shortest vector connecting the two lines. It is obvious that when it is orthogonal to both u_1 and u_2, the segment is the shortest:

$$\begin{cases} (\mathrm{P}_1 + a_1\mathrm{u}_1 - (\mathrm{Q}_1 + a_2\mathrm{u}_2)) \cdot \mathrm{u}_1 = 0 \\ (\mathrm{P}_1 + a_1\mathrm{u}_1 - (\mathrm{Q}_1 + a_2\mathrm{u}_2)) \cdot \mathrm{u}_2 = 0 \end{cases} \tag{5}$$

From the linear equation (5) , the scale factor a_1 and a_2 are solved:

$$\begin{cases} a_1 = \frac{(\mathrm{Q}_1-\mathrm{P}_1)\cdot\mathrm{u}_1 - ((\mathrm{Q}_1-\mathrm{P}_1)\cdot\mathrm{u}_2)(\mathrm{u}_1\cdot\mathrm{u}_2)}{1-(\mathrm{u}_1\cdot\mathrm{u}_2)} \\ a_2 = \frac{((\mathrm{Q}_1-\mathrm{P}_1)\cdot\mathrm{u}_1)(\mathrm{u}_1\cdot\mathrm{u}_2) - (\mathrm{Q}_1-\mathrm{P}_1)\cdot\mathrm{u}_2}{1-(\mathrm{u}_1\cdot\mathrm{u}_2)} \end{cases} \tag{6}$$

Then the vector equation of the shortest line is described as follows:

$$\mathrm{V} = \mathrm{P}_1 + a_1\mathrm{u}_1 - (\mathrm{Q}_1 + a_2\mathrm{u}_2) \tag{7}$$

Hence, the coordinate of the windshield surface point is expressed as:

$$(x,y,z)^t = ((\mathrm{P}_1 + a_1\mathrm{u}_1) + \mathrm{Q}_1 + a_2\mathrm{u}_2)/2 \tag{8}$$

Additionally, the normal of the point on the windshield surface is obtained by:

$$N = (\mathrm{u}_1 + \mathrm{u}_2)/2 \tag{9}$$

When we get the position and normal for every windshield surface point, we can know the reflection property of the windshield. Sometimes, it is very important to know this for the windshield.

D. Error Analysis

The error in our system is mainly caused by the coordinate of P_1 and P_2. We just place the white board perpendicular to axis z (it is easy to ensure that), which will be discussed in next section. Then we get the x, y coordinate of each point on the board by the calibrated projector. Therefore, the main error source of P_1 and P_2 coordinate is the error in the axis

z relative to x, y axes. We assume that P_1 and P_2 are the real coordinates in the world frame and P_1' and P_2' are the calculated coordinates in the world frame shown in Fig.6.

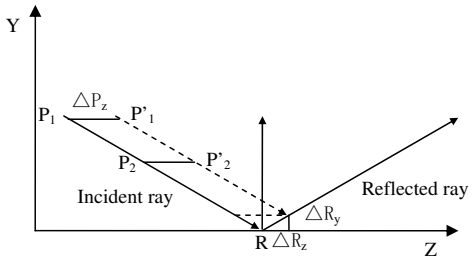

Fig. 6. System measurement error

From Fig.6, we know that the relative displacement of P_1P_1' is equal to P_2P_2'. The unit vector of the incident ray can be defined as:

$$u = \overrightarrow{P_1P_2} / \text{ mod } (\overrightarrow{P_1P_2}) \tag{10}$$

In this case, the measured errors of the point R on the windshield surface in the axis y and axis z, respectively, are

$$R_y = \frac{\Delta P_z}{2\tan\theta}; R_z = \frac{\Delta P_z}{2} \tag{11}$$

Where ΔP_z is the error of the board in axis z; θ is the incident angle; ΔR_y and ΔR_z are the errors of measured point on the windshield surface in the directions y and z.

Because the incident angle for each point on the windshield surface changes very slightly, the error of each point is approximately equal. This means that such error for every point on the windshield can be considered as system error. It also means that the relative distance between every point on the windshield surface is unchanged which show that we can the accurately inspect the 3D shape of the windshield. Overall, the system has high accuracy performance.

III. CALIBRATION

In order to obtain the accurate 3D shape of the windshield, the accurate calibration of the components and system is the key task. In our measurement system, the camera, projector and system all need calibration. A camera is regarded as a pinhole model [12]. The relation between a point in the world frame and its corresponding pixel in the image can be described as follows based on a pinhole model:

$$sI = AFX \tag{12}$$

Where $I = [r, c, 1]^T$ is the homogeneous coordinate of the pixel in the image frame; $X = [x, y, z, 1]^T$ is the homogeneous coordinate of the corresponding point in the world frame; s is a scale factor; F is the extrinsic parameters representing the rotation and translation between the camera frame and world frame; and A is the camera intrinsic parameters matrix and can be written as:

$$A = \begin{bmatrix} \alpha & \gamma & r_0 \\ 0 & \beta & c_0 \\ 0 & 0 & 1 \end{bmatrix} \tag{13}$$

Where r_0 , c_0 are the coordinates of the principal point; α and β are focal lengths along the r and c axes of the image plane; γ is the parameter representing the skew of the two image axes. We calibrate the camera using Zhang's method [12]. The flat checkerboard with size of 15×15 mm placed on different positions and orientations are imaged by the camera shown as in Fig.7.

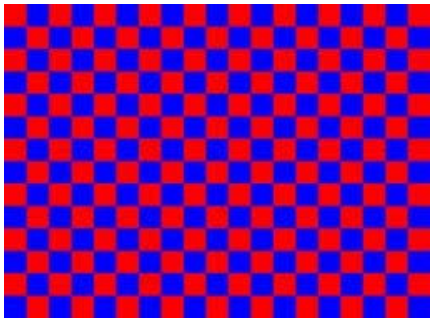

Fig. 7. Checkerboard for calibration

Likewise, a projector also can be regarded as an inverse camera since it projects images instead of capturing them. Therefore, if the corresponding relation between the camera pixel and projector pixel can be obtained, the projector pixel position in the projector image plane can be found. In this case, we can use the same calibration method that is used in camera calibration. The method we use is similar with Zhang's method [13] except that CGLS is used to establish the corresponding relation between the camera pixel and projector pixel instead of CGPS. When the camera and projector are calibrated, the next step is to calibrate the whole inspection system. For this purpose, a uniform world frame for the camera and projector is established base on one calibration image with xy axes on the plane and z axis perpendicular to the plane. In addition, the white board is placed parallel to the xy plane shown as in Fig.8. In this case, the coordinate of every pixel on the board can be computed by equation (3) because each pixel has known parameters z, r and c.

IV. EXPERIMENT AND RESULTS

The experiment setup is shown in Fig.9. one camera(SONY XCD X 710 with FUJINON TV LENS) and one projector (PLUS V339) are mounted on the frame structure made of Alumni T slot. The first experiment is conducted to validate the calibration accuracy. The intrinsic parameters A_c and A_p of the camera and projector are as follows:

$$A_C = \begin{bmatrix} 2713.4 & 0 & 511.5 \\ 0 & 2692 & 383.5 \\ 0 & 0 & 1 \end{bmatrix};$$

$$A_P = \begin{bmatrix} 2437.6 & 0 & 511.5 \\ 0 & 2387.5 & 488.5 \\ 0 & 0 & 1 \end{bmatrix};$$

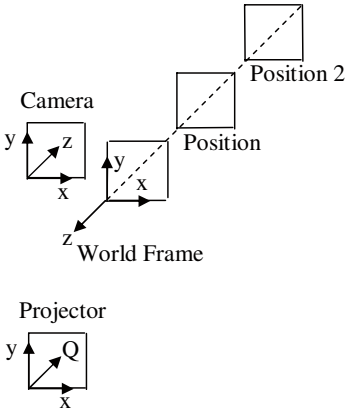

Fig. 8. World coordinate system

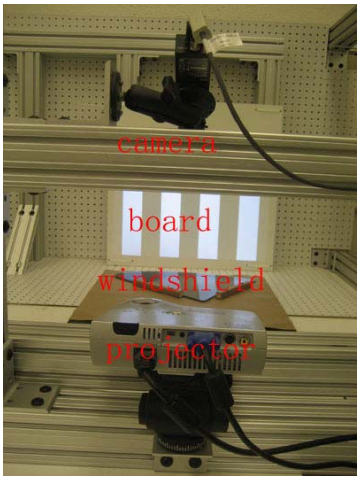

Fig. 9. Experiment setup

$$F_C = \begin{bmatrix} -0.007 & 0.998 & -0.070 & -48.650 \\ 0.873 & 0.040 & 0.487 & -89.950 \\ 0.488 & -0.057 & -0.871 & 720.048 \\ 0 & 0 & 0 & 1 \end{bmatrix};$$

$$F_P = \begin{bmatrix} -0.009 & 0.998 & 0.064 & -89.487 \\ 0.999 & 0.006 & 0.051 & -21.502 \\ 0.050 & 0.065 & -0.997 & 972.512 \\ 0 & 0 & 0 & 1 \end{bmatrix}$$

In our system, we ignore the distortion of the lenses since it is very small. To verify the calibration accuracy, each checkerboard corner is converted to the position in the camera and projector image plane. Then the difference between the converted position and the captured position denotes the error of the calibration as shown in Fig.10. The results demonstrate the error of both camera and projector is within one pixel.

The second experiment is carried out to verify the accuracy of the inspection system. Fig.11 shows the tested CAD model. This CAD model contains 576 triangles. The

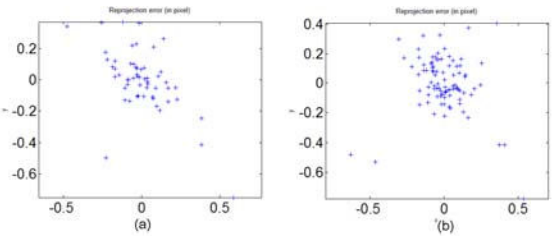

Fig. 10. Calibration error (a) camera (b) projector

windshield is measured to obtained point cloud shown in Fig.12 .

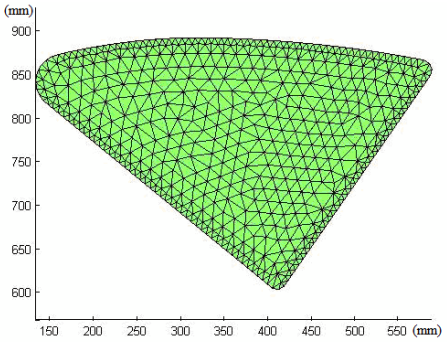

Fig. 11. CAD model

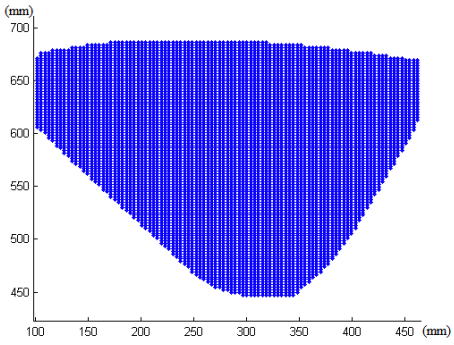

Fig. 12. Measured point cloud

Next, the point cloud is registered with the CAD model by iterative closed point (ICP) algorithm. Shape difference between the CAD model and the tested point cloud can be expressed as a color-coded error map shown in Fig. 13. In addition, the normal of the windshield is also obtained as in Fig.14.

From Fig. 13, we find the error in the boundary is greater than the center region. The reason for that is the center region having more measured points than the boundary which results in the center region has small errors by the ICP registration algorithm. The mean error is 0.32mm and the standard deviation of the result is 0.27mm

The system consistency experiments are also carried out in our lab. The windshield is placed at different positions

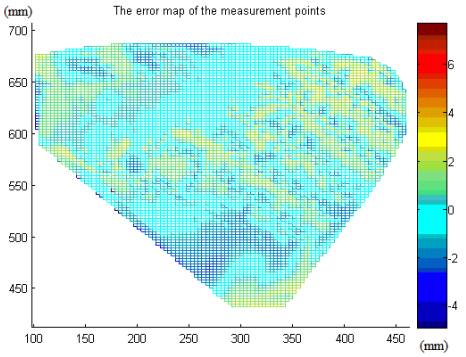

Fig. 13. Error map between point cloud and CAD model

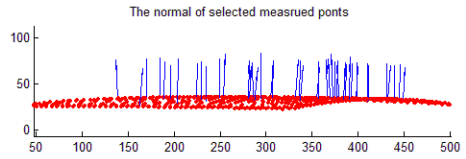

Fig. 14. The normal of windshield

and then inspected by our system. We get the mean error and standard deviation between the point cloud and the CAD model at is calculated at every position, which is represented by e_i and d_i . The experiment is repeated 20 times. The mean error of system consistency is 0.02mm and the stand deviation is 0.08mm.

V. CONCLUSION

In this paper, we propose a new technique for inspecting the shape of a windshield. Different from convention techniques, the windshield dose not need to be painted before measurement.

We placed a planar diffuse source at different positions and captured the distorted patterns separately. In order to achieve high accuracy performance, the vertical and horizontal CGLS patterns were used instead of CGPS. Due to the patterns, the corresponding points on the planar diffuse source can be found. In this case, the incident ray for each point on the windshield surface could be obtained through the corresponding points. The reflected ray can be obtained by camera calibration. We can get not only the surface position but also the surface normal. If we get the normal, the reflective property is known. Last, calibration and system measurement accuracy experiments were conducted. The results demonstrate the method has high accuracy performance.

In the future, ways to measure the windshield transmission distortion will be studied in our lab.

REFERENCES

[1] C. Zhang, N. Xi, and Q. Shi , "Object-orientated Registration Method for Surface Inspection of Automotive Windshields", *IEEE Int Conf. Intelligent Robots and Systems* , Nice French Sept , 2008, pp 3553-3558.

[2] Q, Shi,"Develop rapid 3D surface measurement systems for quality inspection in the manufacturing industry" , *PH.D thesis*, Michigan state university,MI,USA; 2008.

[3] A. C. Sanderson, L. E. Weiss, and S. K. Nayar, "Structured highlight inspection of specular surfaces", *IEEE Trans. Pattern. Anal. Mach. Intell.*, vol.10, 1988, pp. 44-55.

[4] X. Zhang and W. North, "Analysis of 3-D surface waviness on standard artifacts by retroreflective metrology", *Opt. Eng*, vol. 39, 2000, pp 183-186.

[5] T. Bothe, W. Li, C. von Kopylow, and W. P. O. Jptner,"High-resolution 3D shape measurement on specular surfaces by fringe reflection", *In SPIE Proc.on Optical Metrology in Production Engineering*, vol.5457, 2004, pp411-422.

[6] O. A. Skydan, M. J. Lalor, and D. R. Burton, "Three-dimensional shape measurement of non- full-field reflective surfaces", *Appl. Opt.*, vol.44, 2005, pp. 4745-4752.

[7] O. A. Skydan, M. J. Lalor, and D. R. Burton,"3D shape measurement of automotive glass by using a fringe reflection technique", *Meas. Sci. Technol..*, vol. 18, 2007, pp.106-114

[8] Kiyasu S, Hoshino H, Yano K, Fujimura S, "Measurement of the 3-D shape of specular polyhedrons using an M-array coded light source", *IEEE transactions on instrumentation and measurement,*, vol.44,1994, pp. 775-778.

[9] Hongwei Guo, Peng Feng, Tao Tao, "Specular surface measurement by using a moving diffusive structured light source", *Proc. SPIE*, vol.6834,2007.

[10] D. Bergmann, "New approach for automatic surface reconstruction with coded light",*Proceedings of Remote Sensing and Reconstruction for Three-Dimensional Objects and Scenes*, vol.2572, SPIE,1995, pp 2-9.

[11] Linda G. Shapiro, "Computer Vision",Prentice Hall, NJ; 2001.

[12] Z. Zhang, "A flexible new technique for camera calibration", *IEEE Trans on Pattern Analysis and Machine Intelligence*, vol. 22,2000, pp 1330-1334.

[13] S. Zhang and P. S. Huang,"Novel method for structured light system calibration" *Optical Engineering*, vol. 45,2006, pp 1-8.